Superconducting spin valves based on antiferromagnet/superconductor/antiferromagnet heterostructures

G. A. Bobkov,[1] V. M. Gordeeva,[1] Lina Johnsen Kamra,[2,3] Simran Chourasia,[2] A. M. Bobkov,[1]
Akashdeep Kamra,[2] and I. V. Bobkova[1,4]

[1]*Moscow Institute of Physics and Technology, Dolgoprudny, 141700 Moscow Region, Russia*
[2]*Condensed Matter Physics Center (IFIMAC) and Departamento de Física Teórica de la Materia Condensada, Universidad Autónoma de Madrid, E-28049 Madrid, Spain*
[3]*Department of Physics, Massachusetts Institute of Technology, Cambridge, Massachusetts 02139, USA*
[4]*National Research University Higher School of Economics, 101000 Moscow, Russia*

(Received 31 January 2024; accepted 16 April 2024; published 2 May 2024)

Proximity effect at superconductor/antiferromagnet (S/AF) interfaces, which manifests itself as generation of Néel-type triplet correlations, leads to sensitivity of the superconducting critical temperature to the mutual orientation of the AF Néel vectors in AF/S/AF trilayers, which is called the spin-valve effect. Here we predict that the spin-valve effect in AF/S/AF heterostructures crucially depends on the value of the chemical potential of the superconducting interlayer due to the occurrence of the finite-momentum Néel triplet correlations. In addition, we investigate equal-spin-triplet correlations, which appear in AF/S/AF structures for nonaligned Néel vectors of the AFs, and their role in the nonmonotonic dependence of the superconducting critical temperature of the AF/S/AF structure on the mutual orientation of the AF Néel vectors. The influence of impurities on the spin-valve effect is also investigated.

DOI: 10.1103/PhysRevB.109.184504

I. INTRODUCTION

Heterostructures constructed of superconductors and magnetic materials are objects of great interest for superconducting spintronics due to proximity effects occurring in the nanoscale interface regions [1–4]. In particular, magnetic-induced spin-splitting field leads to partial conversion of singlet pairing correlations to triplet ones, which suppresses conventional spin-singlet superconductivity. One of the possible spintronics devices based on such structures is a superconducting spin valve, where the superconducting critical temperature T_c is sensitive to the mutual orientation of the magnetic layer magnetizations (spin-valve effect). In particular, a switching between the superconducting and the normal states, that is the absolute spin-valve effect, can be realized by changing the mutual orientation of the magnetic layers.

Spin valves based on superconductor/ferromagnet (S/F) proximity effect have been widely studied both theoretically and experimentally. The F/S/F structure with insulating ferromagnets was theoretically considered by de Gennes [5], who showed that the average exchange field felt by the superconductor is proportional to $\cos(\phi/2)$, where ϕ is the misorientation angle between F magnetizations. This result predicted the spin-valve effect in such systems: according to it, the critical temperature in the case of parallel (P) magnetizations should be lower than in the antiparallel (AP) configuration, which was later experimentally obtained by Li *et al.* [6].

In trilayers with metallic ferromagnets the physics is more complicated because the singlet and triplet superconducting correlations can also penetrate into the ferromagnetic regions due to the proximity effect. However, such structures (F1/F2/S as well as F/S/F) are also well studied in terms of the spin-valve effect [7–23]. Interestingly, theory for F1/F2/S systems by Fominov *et al.* [12] shows the possibility of both “standard” and “reverse” spin-valve effect (when the critical temperature is lower in the P or AP configuration, respectively) due to constructive or destructive interference of the Cooper pair wave functions reflected from F1/F2 and F2/S interfaces. Besides, the T_c dependence on the misorientation angle might be nonmonotonic with a minimum near $\phi = \pi/2$ [12,14,15,17–19,24] because of generation of the long-range triplet component which provides an additional way of superconductivity suppression in the case of noncollinear magnetizations. Research on the spin-valve-based devices is furthered [25] because, aside from their great scientific interest, they have possible applications towards the creation of nonvolatile magnetic memory elements. The supercurrents passed through these devices can also be spin polarized [26–30], what can then lead to a low-energy spin-transfer torque that can be used to control the magnetization of nanoscale devices.

The dipolar stray fields and GHz frequency magnons in F often cause parasitic detrimental influence in ferromagnet-based spintronic devices including superconducting spin valves. Employing antiferromagnets (AFs) could significantly reduce these problems due to their zero net magnetization and higher magnon frequencies [31–35]. Simultaneously, the zero net magnetization of AFs has long been considered to be an obstacle to the use of antiferromagnets in spintronic devices. However, it was recently shown that the superconducting spin-valve effect can also be realized in three-layer antiferromagnet/superconductor/antiferromagnet (AF/S/AF) structures despite the absence of macroscopic magnetization in the antiferromagnetic layers [36]. In that work the AF/S/AF spin valve with insulating antiferromagnets and fully compensated S/AF interfaces (that is, with zero interface magnetization) was theoretically investigated in Bogoliubov–de Gennes (BdG) framework. It may seem that such a system is invariant towards reversing the direction of the Néel vectors in one of the AFs and, consequently, there is no physical difference between parallel and antiparallel configurations. However, each of the S/AF interfaces generates triplet correlations called Néel triplets [37]. The amplitude of these correlations changes its sign between the adjacent lattice sites in the superconductor in the same way as the magnetic order in the antiferromagnet does. The Néel triplets generated by the both S/AF interfaces may interfere constructively (destructively) inside the superconducting layer, thus suppressing superconductivity more (less) strongly. Therefore, the spin-valve effect is expected even in AF/S/AF heterostructures with fully compensated S/AF interfaces.

In [36] it was obtained that the critical temperature is sensitive to mutual orientation of the Néel vectors of the AFs and complete suppression of T_c, or the absolute spin-valve effect, is achievable. In this work we supplement those results with a more detailed study of $T_c(\phi)$ behavior in various regimes. In particular, it is shown that similar to other important physical effects in S/AF hybrids, such as dependence of the critical temperature on impurity concentration [37,38], magnetic anisotropy of the critical temperature in the presence of spin-orbit coupling [39], and dependence of the critical temperature on the canting angle [40], the physics of spin-valve effect is also very sensitive to the value of the chemical potential μ_S in the superconducting layer. We observed an interesting and nontrivial dependence of T_c on the misorientation angle between the Néel vectors of the AFs. In AF/S/AF structures there is some freedom in determination of the misorientation angle. In [36] the misorientation angle θ was defined as the angle between the Néel vectors of the closest to the S/AF interfaces antiferromagnetic layers. Here we focus on other aspects of physics of AF/S/AF heterostructures and it is more convenient to choose a unified division of the entire AF/S/AF structure into two sublattices and to define the misorientation angle ϕ as the angle between the magnetizations of two antiferromagnets at the same sublattice (see Fig. 1 and the description of the model for further details of the definition). In [36] it was shown that near half-filling, that is at $\mu_S \approx 0$, the critical temperature is always lower for the parallel state corresponding to $\phi = 0$ [$T_c(0) \equiv T_c^{\mathrm{P}}$] than in the antiparallel state corresponding to $\phi = \pi$ [$T_c(\pi) \equiv T_c^{\mathrm{AP}}$]. Please notice that the parallel and antiparallel orientations are defined using the convention followed in this paper. It is explained by the fact that in this case the Néel triplets generated by the both interfaces are effectively summed up and strengthen each other inside the S layer. Here we demonstrate that if we move away from half-filling the opposite result $T_c^{\mathrm{P}} > T_c^{\mathrm{AP}}$ can be realized depending on the width of the S layer. We unveil the physical reason of this phenomenon, which is connected with the generation of finite-momentum Néel triplet pairs [41]. Further, in [36] it was indicated that the dependence $T_c(\phi)$ contains a contribution $\sim\sin^2\phi$, which was ascribed to generation of equal-spin-triplet correlations of conventional, not Néel, character. But near half-filling this contribution was

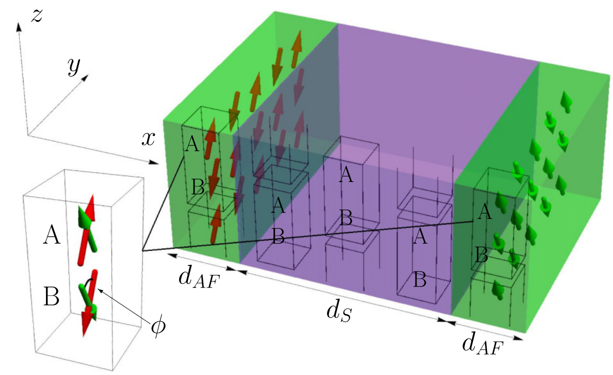

FIG. 1. Sketch of the AF/S/AF system. Red and green arrows show Néel-type magnetizations of the AFs. The unified division into two sublattices with unit cells containing two sites belonging to A and B sublattices is also shown. The misorientation angle ϕ is defined as the angle between the magnetizations of two antiferromagnets at the same sublattice. It is important to note that this definition of the misorientation angle differs from the definition used in [36].

found to be small. Here we investigate equal-spin contribution in more detail, provide its analytical description, and find parameter regions, where it is rather strong and results in the nonmonotonic dependence $T_c(\phi)$. Finally, we discuss the dependence of the spin-valve effect on the presence of impurities in the S layer and demonstrate that the difference $T_c^{\mathrm{P}} - T_c^{\mathrm{AP}}$ is suppressed by impurities due to the sensitivity of the Néel triplet correlations to impurities, but spin-valve effect produced by equal-spin pairs, which can be quantified by the difference $T_c^{\mathrm{P}} + T_c^{\mathrm{AP}} - 2T_c(\phi = \pi/2)$, is not suppressed by impurities in the superconductor.

The paper is organized as follows. In Sec. II we present semianalytical results obtained in the framework of the quasiclassical theory. Section II A is devoted to description of the model of the AF/S/AF trilayer we study and the formalism of the two-sublattice quasiclassical theory applicable to S/AF hybrid structures. In Sec. II B we present some analytical results and discuss the structure of triplet correlations responsible for the spin-valve effect in the AF/S/AF trilayer, while in Sec. II C the dependencies $T_c(\phi)$ obtained in the framework of our quasiclassical theory are provided and discussed. Section III is devoted to the presentation of numerical results obtained in the framework of the BdG approach. Section III A briefly describes the method. In Sec. III B we study the dependence of the spin-valve effect on the value of the chemical potential of the S layer, and Sec. III C is devoted to the influence of impurities on the investigated effect. In Sec. III D we describe the requirements for materials. Section IV contains the conclusions from our work. In the Appendix some technical details of the quasiclassical calculations are provided.

II. QUASICLASSICAL THEORY: STRUCTURE OF TRIPLET CORRELATIONS AND SPIN-VALVE EFFECT

A. Model and method

We consider an AF/S/AF trilayer system with fully compensated interfaces, depicted in Fig. 1. A conventional s-wave singlet superconductor with thickness d_S is sandwiched between two insulating antiferromagnets with the same thicknesses d_{AF}. For simplicity we study a two-dimensional system and employ periodic boundary conditions along the interfacial direction. We introduce a unified division into two sublattices for the entire AF/S/AF system. The misorientation angle ϕ is defined as the angle between the magnetizations of both antiferromagnets at the same sublattice (see Fig. 1). Please note that this definition of the misorientation angle differs from the definition used in [36]. In that paper the misorientation angle θ was defined as the angle between the Néel vectors of the closest to the S/AF interfaces antiferromagnetic layers. Both definitions coincide for odd number of layers in the superconductor, but they differ by π if the number of layers in the superconductor is even.

In order to obtain some analytical results on the structure of superconducting correlations in the S layer, including triplet ones, we investigate the clean case $T_c(\phi)$ dependence in the framework of the two-sublattice quasiclassical theory [37]. The unit cell containing two sites belonging to different sublattices A and B is shown in Fig. 1. The Hamiltonian of the superconducting layer in the two-sublattice representation takes the form

$$\hat{H} = -t \sum_{\langle \boldsymbol{ij}\nu\bar{\nu}\rangle,\sigma} \hat{\psi}^{\nu\dagger}_{\boldsymbol{i}\sigma}\hat{\psi}^{\bar{\nu}}_{\boldsymbol{j}\sigma} + \sum_{\boldsymbol{i},\nu}\left(\Delta^{\nu}_{\boldsymbol{i}}\hat{\psi}^{\nu\dagger}_{\boldsymbol{i}\uparrow}\hat{\psi}^{\nu\dagger}_{\boldsymbol{i}\downarrow} + \mathrm{H.c.}\right) - \mu_{\mathrm{S}}\sum_{\boldsymbol{i}\nu,\sigma}\hat{n}^{\nu}_{\boldsymbol{i}\sigma} + \sum_{\boldsymbol{i}\nu,\alpha\beta}\hat{\psi}^{\nu\dagger}_{\boldsymbol{i}\alpha}\left(\boldsymbol{h}^{\nu}_{\boldsymbol{i}}\boldsymbol{\sigma}\right)_{\alpha\beta}\hat{\psi}^{\nu}_{\boldsymbol{i}\beta}. \quad (1)$$

Here $\boldsymbol{i}$ is the radius vector of a unit cell as a whole, $\nu = A, B$ denotes the two sites in the unit cell corresponding to different sublattices, $\bar{\nu} = B(A)$ if $\nu = A(B)$. $\hat{\psi}^{\nu\dagger}_{\boldsymbol{i}\sigma}$ ($\hat{\psi}^{\nu}_{\boldsymbol{i}\sigma}$) is the creation (annihilation) operator for an electron with spin σ at the site of the unit cell $\boldsymbol{i} = (i_x, i_y)^T$ and sublattice ν. The x and y axes are taken normal to the S/AF interfaces and parallel to them, respectively. $\langle \boldsymbol{ij}\nu\bar{\nu}\rangle$ means summation over the nearest neighbors, t denotes the hopping between adjacent sites, μ_{S} is the electron chemical potential, and $\hat{n}^{\nu}_{\boldsymbol{i}\sigma} = \hat{\psi}^{\nu\dagger}_{\boldsymbol{i}\sigma}\hat{\psi}^{\nu}_{\boldsymbol{i}\sigma}$ is the particle-number operator at the site $(\boldsymbol{i}, \nu)$. $\Delta^{\nu}_{\boldsymbol{i}}$ and $\boldsymbol{h}^{\nu}_{\boldsymbol{i}}$ denote the onsite s-wave pairing and magnetic order parameter at the site $(\boldsymbol{i}, \nu)$, respectively. $\boldsymbol{\sigma} = (\sigma_x, \sigma_y, \sigma_z)^T$ is the vector of Pauli matrices in spin space.

As we consider G-type antiferromagnets, the magnetic order parameter in the left and right AFs can be taken in the form $\boldsymbol{h}^{A(B)}_{\boldsymbol{i}} = +(-)\boldsymbol{h}_{l,r}$. It is assumed that the antiferromagnetism is due to the localized electrons and the amplitude of the onsite magnetization is not influenced by the adjacent metal. Therefore, we do not calculate the magnetic order parameter self-consistently and consider it to have a constant value h in the AF regions and zero value in the S region. For the onsite s-wave pairing in the S $\Delta^{A}_{\boldsymbol{i}} = \Delta^{B}_{\boldsymbol{i}} = \Delta_{\boldsymbol{i}}$. $\Delta_{\boldsymbol{i}}$ is nonzero only in the superconductor.

As all the parameters in the considered problem are slow functions of the lattice site spatial coordinate, we can introduce a continuous spatial variable $\boldsymbol{R}$ instead of the discrete index $\boldsymbol{i}$. Then the two-sublattice formalism allows us to describe the system with the quasiclassical Green's function $\check{g}(\boldsymbol{R}, \boldsymbol{p}_F, \omega_m)$, which is an 8×8 matrix in the direct product of spin, particle-hole, and sublattice spaces [$\boldsymbol{p}_F$ is the electron momentum at the Fermi surface, $\omega_m = \pi T(2m+1)$ is the fermionic Matsubara frequency].

Let us choose the coordinate system $\boldsymbol{e}_x, \boldsymbol{e}_y, \boldsymbol{e}_z$, so that $\boldsymbol{e}_x$ is parallel to $\boldsymbol{h}_l \times \boldsymbol{h}_r$, $\boldsymbol{e}_z$ is parallel to $\boldsymbol{h}_l + \boldsymbol{h}_r$, and $x = 0$ corresponds to the middle of the S layer. Then $\boldsymbol{h}_{l,r}$ can be written in the form

$$\boldsymbol{h}_l = h\begin{pmatrix} 0 \\ \sin(\phi/2) \\ \cos(\phi/2)\end{pmatrix}, \quad \boldsymbol{h}_r = h\begin{pmatrix} 0 \\ -\sin(\phi/2) \\ \cos(\phi/2)\end{pmatrix}. \quad (2)$$

The quasiclassical Green's function in the superconductor obeys the following Eilenberger equation in the ballistic limit [37]:

$$[(i\omega_m\tau_z + \mu_{\mathrm{S}} + \tau_z\check{\Delta}(\boldsymbol{R}) - \boldsymbol{h}(x)\boldsymbol{\sigma}\rho_z\tau_z a)\rho_x, \check{g}] + i\boldsymbol{v}_F\nabla\check{g} = 0, \quad (3)$$

where $\boldsymbol{h}(x) = \boldsymbol{h}_l\delta(x + d_{\mathrm{S}}/2) + \boldsymbol{h}_r\delta(x - d_{\mathrm{S}}/2)$, $\boldsymbol{v}_F$ is the Fermi velocity for the trajectory $\boldsymbol{p}_F$, τ_i and ρ_i are Pauli matrices in particle-hole and sublattice spaces, respectively, $\check{\Delta}(\boldsymbol{R}) = \Delta(\boldsymbol{R})\tau_x$. The term proportionate to $\boldsymbol{h}_{l,r}\boldsymbol{\sigma}a\delta(x \pm d_{\mathrm{S}}/2)$ accounts for the exchange field at the left and right S/AF interfaces $x = \mp d_{\mathrm{S}}/2$, a is the lattice constant of the superconductor along the x direction.

As we consider the system translationally invariant along the S/AF interfaces, the Green's function depends only on the x coordinate, normal to the interfaces. Then the term $i\boldsymbol{v}_F\nabla\check{g}$ in (3) is reduced to $iv_{F,x}d\check{g}/dx$. We define the Green's functions corresponding to the trajectories, incident to the right S/AF interface and reflected from it, respectively, as $\check{g}_+(x) \equiv \check{g}(x, v)$ and $\check{g}_-(x) \equiv \check{g}(x, -v)$, where for brevity we introduce the notation $v \equiv |v_{F,x}|$. In addition to the Eilenberger equation (3), the quasiclassical Green's function for a given trajectory $\check{g}_{+(-)}(x)$ obeys the normalization condition

$$[\check{g}_{+(-)}(x)]^2 = 1 \quad (4)$$

and the boundary conditions at the S/AF interfaces $x = \mp d_{\mathrm{S}}/2$, which, due to the symmetrically chosen coordinate system, are reduced to one boundary condition at one of the interfaces (for the following calculations we take the right interface $x = d_{\mathrm{S}}/2$).

In the problem under consideration the S layer width d_{S} is assumed to be much smaller than the superconducting coherence length $\xi_{\mathrm{S}} = v_F/2\pi T_{c0}$, where T_{c0} is the superconducting bulk critical temperature. Therefore, we can consider the superconducting order parameter in the S region spatially constant: $\Delta(\boldsymbol{R}) \approx \Delta$. The explicit structure of the Green's function in the particle-hole space takes the form

$$\check{g} = \begin{pmatrix} \hat{g} & \hat{f} \\ \hat{\tilde{f}} & \hat{\tilde{g}}\end{pmatrix}_\tau, \quad (5)$$

where all the components are 4×4 matrices in the direct product of spin and sublattice spaces. As we study the system at temperatures close to the critical temperature, the Eilenberger equation (3) can be linearized with respect to Δ/T_c. The diagonal components $\hat{g}$ and $\hat{\tilde{g}}$ are to be calculated in the normal state of the superconductor and the anomalous components $\hat{f}$ and $\hat{\tilde{f}}$ are of the first order with respect to Δ/T_c.

For the normal-state Green's function

$$\check{g}^N = \begin{pmatrix} \hat{g} & 0 \\ 0 & \hat{\tilde{g}}\end{pmatrix}_\tau \quad (6)$$

the Eilenberger equation (3) takes the form

$$[[i\omega_m\tau_z + \mu_S - \boldsymbol{h}(x)\boldsymbol{\sigma}\rho_z\tau_z a]\rho_x, \check{g}^N] + iv_{F,x}\frac{d}{dx}\check{g}^N = 0 \quad (7)$$

and leads to the following boundary condition at $x = d_S/2$ (see the Appendix):

$$\delta\check{g}^N \equiv \check{g}^N_-(x = d_S/2) - \check{g}^N_+(x = d_S/2) = \frac{2\tau_z}{v}\left[a\boldsymbol{h}_r\boldsymbol{\sigma}\rho_y, \frac{\hat{g}_+(x = d_S/2) + \hat{g}_-(x = d_S/2)}{2}\right]. \quad (8)$$

The detailed calculation of $\check{g}^N$, as well as some extra conditions on it resulting from symmetry, are presented in the Appendix. Let us define the following expansions of $\hat{g}$, $\hat{f}$, $\hat{\tilde{f}}$, and $\hat{\tilde{g}}$ over the Pauli matrices in the sublattice space and over the direct product of Pauli matrices in spin and sublattice spaces:

$$\hat{g} = \sum_\alpha \rho_\alpha \hat{g}_\alpha, \quad \hat{g} = \sum_{\alpha,\beta}\sigma_\alpha\rho_\beta g_{\alpha\beta}, \quad (9)$$

and similarly for $\hat{f}$, $\hat{\tilde{f}}$, and $\hat{\tilde{g}}$. The symmetry also gives us the following relation between $\check{g}_-(x)$ and $\check{g}_+(-x)$ (see Appendix for details of the derivation):

$$\begin{aligned}
\check{g}_{0\alpha,-}(x) &= \check{g}_{0\alpha,+}(-x),\\
\check{g}_{x\alpha,-}(x) &= -\check{g}_{x\alpha,+}(-x),\\
\check{g}_{y\alpha,-}(x) &= -\check{g}_{y\alpha,+}(-x),\\
\check{g}_{z\alpha,-}(x) &= \check{g}_{z\alpha,+}(-x),
\end{aligned} \quad (10)$$

where

$$\check{g}_{\beta\alpha,+(-)} \equiv \begin{pmatrix} g_{\beta\alpha,+(-)} & f_{\beta\alpha,+(-)} \\ \tilde{f}_{\beta\alpha,+(-)} & \tilde{g}_{\beta\alpha,+(-)} \end{pmatrix}. \quad (11)$$

Therefore, in the following text we write the expressions only for $\check{g}_+(x) \equiv \check{g}(x)$. The solution for the particle component of the normal-state Green's function takes the form

$$\begin{aligned}
\hat{g} = \operatorname{sgn}\omega_m[&g_{0x}\sigma_0\rho_x + g_{x0}\sigma_x\rho_0\\
&+ B\sigma_y(i\rho_y\sinh\kappa x + \rho_z\operatorname{sgn}v_{F,x}\cosh\kappa x)\\
&+ A\sigma_z(i\rho_z\operatorname{sgn}v_{F,x}\sinh\kappa x - \rho_y\cosh\kappa x)],
\end{aligned} \quad (12)$$

where $\kappa = 2(i\mu_S - \omega_m)/v$ and the coefficients g_{0x}, g_{x0}, A, and B are found from the normalization condition (4) and the boundary condition (8) and take the form (see Appendix for the derivation)

$$\begin{aligned}
g_{0x} &= \frac{1}{\sqrt{(1+\gamma_a^2)(1+\gamma_b^2)}},\\
g_{x0} &= \frac{\gamma_a\gamma_b}{\sqrt{(1+\gamma_a^2)(1+\gamma_b^2)}},\\
A &= \frac{\gamma_a}{\sqrt{(1+\gamma_a^2)(1+\gamma_b^2)}},\\
B &= \frac{\gamma_b}{\sqrt{(1+\gamma_a^2)(1+\gamma_b^2)}},
\end{aligned} \quad (13)$$

where $\gamma_a = 2ah_z/[v\sinh(\kappa d_S/2)]$, $\gamma_b = 2iah_y/[v\cosh(\kappa d_S/2)]$, $h_{y,z} \equiv (\boldsymbol{h}_l)_{y,z}$. The hole component $\hat{\tilde{g}}$ is obtained from (12) by the relation

$$\hat{\tilde{g}}(\omega_m, \boldsymbol{h}_r, \mu_S) = \hat{g}(-\omega_m, -\boldsymbol{h}_r, \mu_S). \quad (14)$$

The anomalous Green's function $\hat{f}$ is found from the linearized with respect to Δ/T_c Eilenberger equation

$$\{[i\omega_m - \boldsymbol{h}(x)\boldsymbol{\sigma}\rho_z a]\rho_x, \hat{f}\} + \mu_S[\rho_x, \hat{f}] + \Delta(\rho_x\hat{\tilde{g}} - \hat{g}\rho_x) + iv_{F,x}\frac{d}{dx}\hat{f} = 0, \quad (15)$$

where $\{F_1, F_2\} = F_1F_2 + F_2F_1$ means anticommutator. And the boundary condition

$$\delta\hat{f} \equiv \hat{f}_-(x = d_S/2) - \hat{f}_+(x = d_S/2) = \frac{2}{v}\left\{a\boldsymbol{h}_r\boldsymbol{\sigma}\rho_y, \frac{\hat{f}_+(x = d_S/2) + \hat{f}_-(x = d_S/2)}{2}\right\}. \quad (16)$$

The details of the calculation of $\hat{f}$ are presented in the Appendix. It is convenient to define the following 2×2 matrices in the sublattice space:

$$\begin{aligned}
\hat{G}_0 &= \Delta(\hat{g}_0 - \hat{\tilde{g}}_0),\\
\hat{G}_x &= \Delta(\hat{g}_x - \hat{\tilde{g}}_x),\\
\hat{G}_y &= -i\Delta(\hat{g}_y + \hat{\tilde{g}}_y),\\
\hat{G}_z &= i\Delta(\hat{g}_z + \hat{\tilde{g}}_z).
\end{aligned} \quad (17)$$

Let us write the following expansions up to the first order with respect to x for the matrices (17): $\hat{G}_\beta = \sum_\alpha \sigma_\alpha G_{\alpha\beta}$, $\hat{G}_{y,z} = \hat{G}^0_{y,z} + \hat{G}'_{y,z}x$. Then in the linear order with respect to x/ξ_S the solution for the anomalous Green's function takes the form $\hat{f} = \sum_{\alpha,\beta}\sigma_\alpha\rho_\beta f_{\alpha\beta}$ with the following nonzero components:

$$\begin{aligned}
f_{00} &= A_0\frac{2\omega_m}{v}x\operatorname{sgn}v_{F,x},\\
f_{0x} &= -A_0 + \frac{G_{0x}}{2i\omega_m},\\
f_{xx} &= -B_x\frac{2\omega_m}{v}x,\\
f_{yy} &= \left(C_y\frac{2\mu_S}{v} + \frac{G'_{yy}}{2i\mu_S}\right)x,\\
f_{yz} &= \operatorname{sgn}v_{F,x}\left[C_y + \frac{1}{2i\mu_S}\left(-G^0_{yz} + \frac{v}{2\mu_S}G'_{yy}\right)\right],\\
f_{zy} &= D_z + \frac{1}{2i\mu_S}\left(G^0_{zy} + \frac{v}{2\mu_S}G'_{zz}\right),\\
f_{zz} &= -x\operatorname{sgn}v_{F,x}\left(D_z\frac{2i\mu_S}{v} - \frac{G'_{zz}}{2i\mu_S}\right),
\end{aligned} \quad (18)$$

where the coefficients A_0, B_x, C_y, and D_z are obtained from the boundary condition (16) and explicitly written in the Appendix.

The critical temperature for each value of the misorientation angle ϕ is calculated from the self-consistency equation

$$\Delta(x) = \int\frac{d\Omega}{4\pi}i\pi\lambda T_c\sum_{\omega_m}f_{0x}(x), \quad (19)$$

where $\int \frac{d\Omega}{4\pi}$ means averaging over the Fermi surface and λ is the dimensionless coupling constant. The amplitude of onsite singlet correlations f_{0x} is spatially constant in the first order with respect to x.

B. Structure of triplet correlations

Now our goal is to discuss the results for the dependence $T_c(\phi)$ in the framework of the quasiclassical theory. First, let us analyze the expression for the full anomalous Green's function in order to find out the types of triplet correlations that different parts of this expression correspond to. It can be written in the form

$$\hat{f} = \hat{f}_0\sigma_0 + \hat{f}_l \boldsymbol{h}_{\text{eff},l}\boldsymbol{\sigma} + \hat{f}_r \boldsymbol{h}_{\text{eff},r}\boldsymbol{\sigma} + \hat{f}_{\text{cross}}(\boldsymbol{h}_{\text{eff},l} \times \boldsymbol{h}_{\text{eff},r})\boldsymbol{\sigma}, \tag{20}$$

where the amplitudes $\hat{f}_i$ are matrices in the sublattice space and we introduce the combination $\boldsymbol{h}_{\text{eff},l(r)} = \boldsymbol{h}_{l(r)}a/d_S$, which is called effective exchange field and physically corresponds to the averaging of the interface exchange field over the whole width d_S of the S layer. Further, we also use the absolute value of the effective exchange field $h_{\text{eff}} \equiv ha/d_S$. The amplitudes $\hat{f}_l$ and $\hat{f}_r$ contain only $\rho_{y,z}$ contributions, which means they are correlations of the Néel type. On the contrary, the cross product amplitude $\hat{f}_{\text{cross}}$ contains only ρ_x contribution and, consequently, corresponds to conventional onsite equal-spin even-momentum odd-frequency triplet correlations. The cross-product correlations are maximal at $\phi \approx \pi/2$. To the leading order with respect to d_S/ξ_S the amplitude $\hat{f}_{\text{cross}}$ takes the form

$$\hat{f}_{\text{cross}} = -\frac{2\Delta x d_S \hat{\rho}_x}{v^2}\left(\frac{\text{sgn}\omega_m}{\sqrt{(\omega_m - i\mu_S)^2 + 4h_{\text{eff},z}^2}} - \frac{\text{sgn}\omega_m}{\sqrt{(\omega_m + i\mu_S)^2 + 4h_{\text{eff},z}^2}}\right), \tag{21}$$

where $h_{\text{eff},z} = h_{\text{eff}}\cos\phi/2$. It is seen that $\hat{f}_{\text{cross}}$ is of the first order with respect to d_S/ξ_S and, therefore, is not pronounced in structures with thin S layers. This behavior differs from the behavior of $\hat{f}_{l,r}$, which remain finite at $d_S/\xi_S \to 0$ with $\hat{f}_l = \hat{f}_r$, what means that for the thin S layers the Néel correlations are only determined by the vector sum of the effective exchange fields produced by the both S/AF interfaces, that is indeed the resulting effective exchange field $\propto\cos\phi/2$, as it was reported for ferromagnets [5].

Moreover, in the framework of the quasiclassical approximation $\hat{f}_{\text{cross}}$ is an odd function of μ_S and consequently $\hat{f}_{\text{cross}} = 0$ at $\mu_S = 0$. It is in agreement with the smallness of the $\sin^2\phi$ contribution in [36], where the case $\mu_S = 0$ was considered and, therefore, the equal-spin-triplet correlations could contribute to this term only beyond the quasiclassical approximation.

C. Dependence of the critical temperature on the misorientation angle

Figures 2 and 3 demonstrate the dependence of the critical temperature on the misorientation angle ϕ. In the limit of thin S layer the influence of the Néel exchange field of the AFs

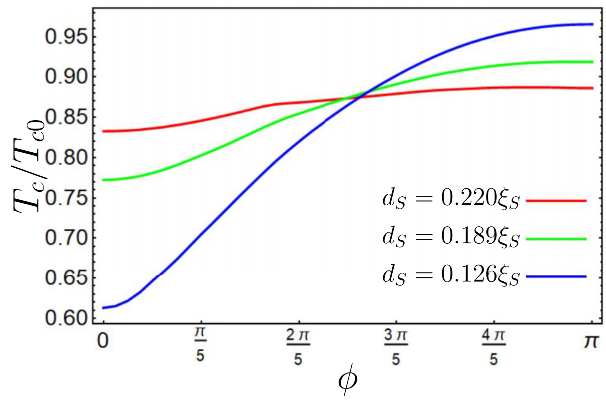

FIG. 2. $T_c(\phi)$ for the AF/S/AF structure in the framework of the quasiclassical approach for fixed $h_{\text{eff}} = T_{c0}$ and different d_S. $\mu_S = T_{c0}$. T_c is measured in units of the superconducting bulk critical temperature T_{c0} throughout the text.

on the S layer is determined by the effective exchange field $h_{\text{eff}} = ha/d_S$. That is, the narrower the S layer is, the stronger effective exchange it feels due to the proximity effect with the antiferromagnets. Figure 2 shows $T_c(\phi)$ for a fixed h_{eff}. The spin-valve effect is well pronounced in all the results in this subsection. The suppression of the critical temperature is maximal at $\phi = 0$ according to the dependence of the effective exchange field on the misoriention angle, which is $2h_{\text{eff}}\cos(\phi/2)$. Thus, here we reached agreement with the expected relation $T_c(\phi = 0) < T_c(\phi = \pi)$.

Figure 2 shows that the valve effect is reduced for larger superconducting width d_S: the T_c suppression becomes weaker at $\phi = 0$ and increases at $\phi = \pi$. This general trend is physically clear. From physical considerations it follows that in the limit $d_S \gg \xi_S$ the valve effect should disappear because the two S/AF interfaces do not feel each other and the superconductivity suppression at each of them does not depend on the direction of the Néel vector. On the contrary, for the thinnest superconductors $d_S \ll \xi_S$ the critical temperature is not suppressed from its bulk value at $\phi = \pi$ due to the exact compensation of the Néel triplets generated at the both interfaces. Therefore, at $\phi = \pi$ the maximal value of the critical temperature is reached for the thinnest S layers with $d_S \ll \xi_S$,

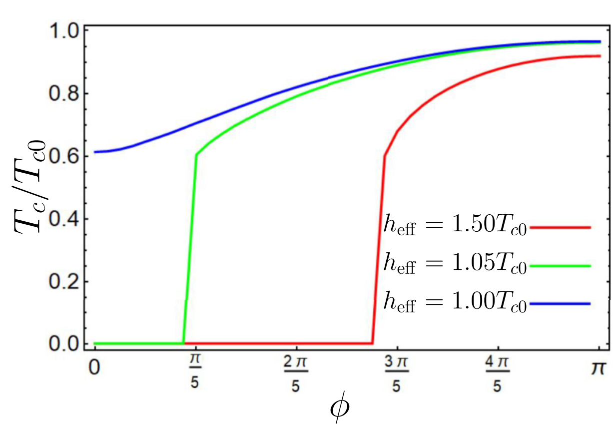

FIG. 3. $T_c(\phi)$ for a fixed $d_S = 0.126\xi_S$ and different h_{eff}. For larger values of h_{eff} the spin-valve effect is absolute: $\mu_S = T_{c0}$.

at larger d_S the critical temperature is lower due to the uncorrelated superconductivity suppression by the Néel exchange field at the S/AF interfaces separately.

Another feature of the results presented in Fig. 2 is the following. For short superconducting interlayers (blue and green curves) the $T_c(\phi)$ dependence is smooth, but for wider d_S the distortion in the vicinity $\phi = \pi/2$ is seen. This is the manifestation of the cross-product term $\sim \boldsymbol{h}_l \times \boldsymbol{h}_r$, which influences singlet correlations with the maximal effect at $\phi = \pi/2$. At $d_S/\xi_S \to 0$ this term disappears, and all the effect of the antiferromagnets on the S layer is described by the total effective exchange field $2h_{\rm eff}\cos\phi/2$. For this reason in the framework of our analytical first-order approximation with respect to d_S/ξ_S it is not possible to obtain more pronounced signatures of these correlations (in the form of dips): higher orders of d_S/ξ_S need to be taken into account. We demonstrate more pronounced dip features at the dependence $T_c(\phi)$ in the framework of the BdG approach below. From our quasiclassical theory it follows that at $h_{\rm eff} \ll T_c$ the dependence $T_c(\phi)$ takes the form $T_c = T_{c,\parallel} + \Delta T_{c,\parallel}\cos\phi + \Delta T_{c,\perp}\sin^2\phi$, as it was phenomenologically proposed in [36]. Here $T_{c,\parallel} = [T_c(0) + T_c(\pi)]/2$, $\Delta T_{c,\parallel} = [T_c(0) - T_c(\pi)]/2$, $\Delta T_{c,\perp} = T_c(\pi/2) - T_{c,\parallel}$. However, at higher $h_{\rm eff}$ plots in Fig. 2 show a clear deviation from this formula, due to the fact that the contributions of higher powers of $(\boldsymbol{h}_{{\rm eff},l}\boldsymbol{h}_{{\rm eff},r})$ and $h_{{\rm eff},z(y)}$ become more significant.

Figure 3 demonstrates that for the system under consideration the absolute spin-valve effect, that is the full suppression of superconducting state for a range of misorientation angles, is also possible. This result is in agreement with the one presented in [36].

III. BOGOLIUBOV–DE GENNES APPROACH: DEPENDENCE OF THE SPIN-VALVE EFFECT ON CHEMICAL POTENTIAL AND IMPURITIES

A. Method

The system is described by a tight-binding Hamiltonian (1), but for the Bogoliubov–de Gennes calculations [42] it is convenient to get rid of sublattices:

$$\hat{H} = -t\sum_{\langle \boldsymbol{ij}\rangle,\sigma}\hat{\psi}^\dagger_{\boldsymbol{i}\sigma}\hat{\psi}_{\boldsymbol{j}\sigma} + \sum_{\boldsymbol{i}}(\Delta_{\boldsymbol{i}}\hat{\psi}^\dagger_{\boldsymbol{i}\uparrow}\hat{\psi}^\dagger_{\boldsymbol{i}\downarrow} + \text{H.c.}) - \mu\sum_{\boldsymbol{i},\sigma}\hat{n}_{\boldsymbol{i}\sigma} + \sum_{\boldsymbol{i},\alpha\beta}\hat{\psi}^\dagger_{\boldsymbol{i}\alpha}(\boldsymbol{h}_{\boldsymbol{i}}\boldsymbol{\sigma})_{\alpha\beta}\hat{\psi}_{\boldsymbol{i}\beta}. \quad (22)$$

Here $\hat{\psi}^\dagger_{\boldsymbol{i}\sigma}$ ($\hat{\psi}_{\boldsymbol{i}\sigma}$) is the creation (annihilation) operator for an electron with spin σ at the site with the radius vector $\boldsymbol{i} = (i_x, i_y)^T$. $\langle \boldsymbol{ij}\rangle$ means summation over the nearest neighbors, $\hat{n}_{\boldsymbol{i}\sigma} = \hat{\psi}^\dagger_{\boldsymbol{i}\sigma}\hat{\psi}_{\boldsymbol{i}\sigma}$ is the particle-number operator at the site $\boldsymbol{i}$. $\Delta_{\boldsymbol{i}}$ and $\boldsymbol{h}_{\boldsymbol{i}}$ denote the onsite s-wave pairing and magnetic order parameter at the site $\boldsymbol{i}$, respectively. The Néel exchange field can be taken in the form $\boldsymbol{h}_{\boldsymbol{i},l} = (-1)^{i_x+i_y}\boldsymbol{h}_l$ and $\boldsymbol{h}_{\boldsymbol{i},r} = (-1)^{i_x+i_y}\boldsymbol{h}_r$ in the left and the right AF regions, respectively. It is worth noting that in the present section the considered AF insulator is also described by hopping Hamiltonian (22). As a result it has a finite band gap such that there is a leakage of the electronic wave functions into the AFs. In fact, the wave functions penetrate to two to three sites. This is in contrast with the ideal antiferromagnetic insulators considered in Ref. [36] and the quasiclassical theory above.

We diagonalize the Hamiltonian (22) by the Bogoliubov transformation:

$$\hat{\psi}_{\boldsymbol{i}\sigma} = \sum_n \left(u^{\boldsymbol{i}}_{n\sigma}\hat{b}_n + v^{\boldsymbol{i}*}_{n\sigma}\hat{b}^\dagger_n\right), \quad (23)$$

where $\hat{b}^\dagger_n$ ($\hat{b}_n$) are the creation (annihilation) operators of Bogoliubov quasiparticles. Then the resulting Bogoliubov–de Gennes equations take the form

$$-\mu u^{\boldsymbol{i}}_{n,\sigma} - t\sum_{\boldsymbol{j}\in\langle \boldsymbol{i}\rangle} u^{\boldsymbol{j}}_{n,\sigma} + \sigma\Delta_{\boldsymbol{i}}v^{\boldsymbol{i}}_{n,-\sigma} + (\boldsymbol{h}_{\boldsymbol{i}}\boldsymbol{\sigma})_{\sigma\alpha}u^{\boldsymbol{i}}_{n,\alpha} = \varepsilon_n u^{\boldsymbol{i}}_{n,\sigma},$$
$$-\mu v^{\boldsymbol{i}}_{n,\sigma} - t\sum_{\boldsymbol{j}\in\langle \boldsymbol{i}\rangle} v^{\boldsymbol{j}}_{n,\sigma} + \sigma\Delta^*_{\boldsymbol{i}}u^{\boldsymbol{i}}_{n,-\sigma} + (\boldsymbol{h}_{\boldsymbol{i}}\boldsymbol{\sigma}^*)_{\sigma\alpha}v^{\boldsymbol{i}}_{n,\alpha} = -\varepsilon_n v^{\boldsymbol{i}}_{n,\sigma}, \quad (24)$$

where $\boldsymbol{j}\in\langle \boldsymbol{i}\rangle$ means summation over the nearest neighbors $\boldsymbol{j}$ of the site $\boldsymbol{i}$ and ε_n are the eigenstate energies of the Bogoliubov quasiparticles. The superconducting order parameter in the S layer is calculated self-consistently:

$$\Delta_{\boldsymbol{i}} = g\langle\hat{\psi}_{\boldsymbol{i}\downarrow}\hat{\psi}_{\boldsymbol{i}\uparrow}\rangle = g\sum_n\left(u^{\boldsymbol{i}}_{n,\downarrow}v^{\boldsymbol{i}*}_{n,\uparrow}(1-f_n) + u^{\boldsymbol{i}}_{n,\uparrow}v^{\boldsymbol{i}*}_{n,\downarrow}f_n\right), \quad (25)$$

where g is the coupling constant. The quasiparticle distribution function is assumed to be the equilibrium Fermi distribution $f_n = \langle b^\dagger_n b_n\rangle = 1/(1+e^{\varepsilon_n/T})$.

Since the simulations can only deal with a small number of lattice sites, it is typical in the BdG approach to employ rescaled parameters that respect the hierarchy of energy scales [42], but do not completely mimic an actual material. For example, in a realistic material, we expect $t \sim 1000T_{c0}$. However, this choice would necessitate the numerical evaluation of eigenenergies with an impossibly high precision. Thus, we choose $T_{c0} \sim (0.01 - 0.1)t$ and $h_{\rm eff} = ha/d_S \sim T_{c0}$. Our analysis then faithfully reproduces realistic systems in which the essential physics depends on the relative strengths of h and T_{c0}, but not on t in consistence with the quasiclassical limit $t \gg T_{c0}$.

B. Dependence of the spin-valve effect on the chemical potential

In this subsection, applying the described technique, we investigate the influence of the chemical potential on the dependence $T_c(\phi)$. In [36] it was demonstrated that at small $h \ll (\mu_S, t)$ (which means that $h_{\rm eff}/\mu_S < h/\mu_S$ is also small) the spin-valve effect is negligible with respect to the effect observed at half-filling $\mu_S = 0$. This is due to the fact that away from half-filling, that is at $\mu_S \gtrsim T_{c0}$, the amplitude of the Néel triplets, mediating the spin-valve effect, is $\sim h_{\rm eff}/\mu_S$ [38]. However, in relation to real systems the both cases $h > \mu_S$ and $h < \mu_S$ can be realized. Therefore, the parameter region $h_{\rm eff} \sim \mu_S$ looks reasonable and also requires investigation. Here we demonstrate that the spin-valve effect persists in this regime. Moreover, in contrast to the case $\mu_S = 0$, where the relation $T_c(0) < T_c(\pi)$ always holds, at larger μ_S the relation between $T_c(0)$ and $T_c(\pi)$ can be opposite. Below we demonstrate this result and discuss its physical reasons.

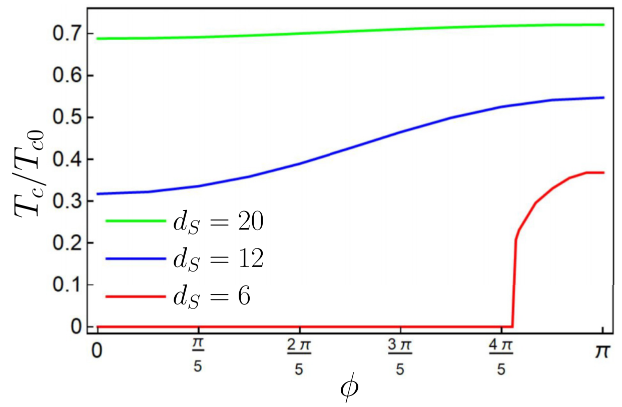

FIG. 4. $T_c(\phi)$ for the AF/S/AF structure in the framework of BdG approach at half-filling $\mu_S = 0$. Different curves correspond to different d_S, $d_{AF} = 4$ (all widths are measured in the number of monolayers), $\mu_{AF} = 0$, $h = 0.5t$, $T_{c0} = 0.07t$.

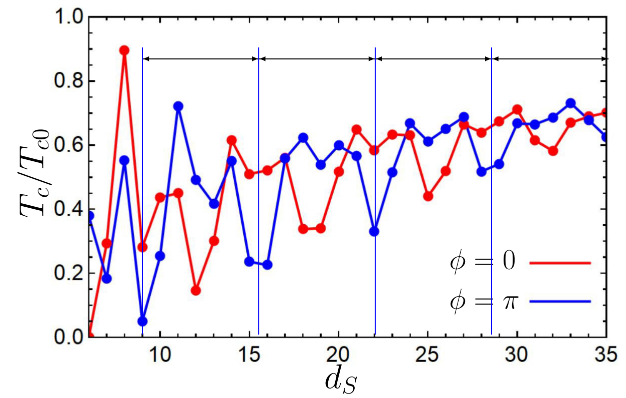

FIG. 6. $T_c(0)$ and $T_c(\pi)$ as functions of d_S at $\mu_S = 0.9t$. $d_{AF} = 4$, $\mu_{AF} = 0$, $h = t$, $T_{c0} = 0.03t$. $h_{eff} = ha/d_S \ll \mu_S$, consequently for this set of parameters $L_{osc} = \pi v_F/\mu_S \approx 7$, what is in agreement with the data: four periods [minima $T_c(d_S)$ for $\phi = \pi$] are shown on the plot by vertical blue lines, so $L_{osc} = \frac{35-9}{4} = 6.5$. The small local minima inside some periods are caused by Friedel oscillations due to unrealistic small number of sites used in the BdG aproach.

In this subsection we assume no impurities in the S layer. Then the translational invariance allows us to consider the cluster infinite along the interfacial direction and solve a one-dimensional (1D) problem for a system with the width $W = d_{AF} + d_S + d_{AF}$ along the x direction. The dependencies $T_c(\phi)$ at $\mu_S = 0$ and $\mu_S = 0.2t$ are shown in Figs. 4 and 5, respectively. For the data presented in these figures $\xi_S = v_F/2\pi T_c \approx 6$ monolayers. We can observe that at $\mu_S = 0$ the results are in agreement with our quasiclassical results presented in the previous section and also they are in agreement with [36]. The relation $T_c(0) < T_c(\pi)$ is fulfilled for all considered values of d_S. However, as it is seen from Fig. 5, at larger μ_S the relation between $T_c(0)$ and $T_c(\pi)$ depends on the value of d_S and opposite cases can be realized. The reason is the finite momentum, acquired by the Néel triplet Cooper pairs [41] in systems with broken translational invariance via the umklapp scattering processes at the S/AF interfaces. Due to the finite momentum of the Néel triplet Cooper pairs their wave function oscillates in the S layer with the period $L_{osc} = \pi v_F/|\mu_S|$. Depending on the width of the S layer d_S the Néel triplets generated by the opposite S/AF interfaces can interfere constructively or destructively in the S layer, which manifests itself in the oscillating behavior of the resulting Néel triplet amplitude for a given ϕ upon varying d_S. This physical picture is further supported by the demonstration of the dependence of $T_c(0, \pi)$ on d_S presented in Fig. 6. The oscillations of the difference $T_c(\pi) - T_c(0)$ with the period L_{osc} are clearly seen.

The other feature worth mentioning is the nonmonotonicity of the curves in Fig. 5. The dip in the critical temperature at ϕ close to $\pi/2$ can be explained by generating of equal-spin-triplet correlations determined by $\boldsymbol{h}_l \times \boldsymbol{h}_r$. These correlations are not of sign-changing Néel type and are usual equal-spin-triplet correlations. The dip can be clearly seen for $d_S = 13$ monolayers. For lower values of the S width the equal-spin-triplet correlations are too weak to result in the pronounced dip feature because they vanish at $d_S/\xi_S \ll 1$ [see Eq. (21)]. For some higher values of d_S the influence of the equal-spin-triplet correlations can be superimposed by the interference effects due to the finite-momentum Néel triplet pairing, which also mask their effect.

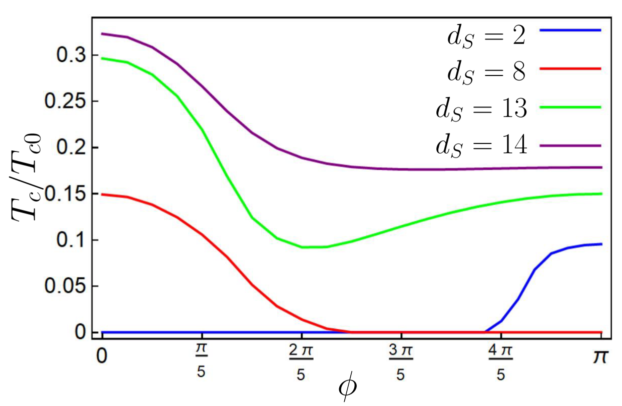

FIG. 5. $T_c(\phi)$ for the AF/S/AF structure in the framework of BdG approach at $\mu_S = 0.2t$. Different curves correspond to different d_S, $d_{AF} = 4$, $\mu_{AF} = 0$, $h = 0.5t$, $T_{c0} = 0.07t$.

C. Dependence of the spin-valve effect on impurities

Now we discuss the influence of impurities in the S region on the $T_c(\phi)$ dependence and spin-valve effect. The impurities are modeled as random changes of the chemical potential μ_S at each site of the superconductor:

$$\mu_i = \mu_S + \delta\mu_i, \quad \delta\mu_i \in [-\delta\mu, \delta\mu], \tag{26}$$

which break the translational invariance along the interface. For this reason we now investigate the 2D cluster with the previously defined width W and finite length L under periodic boundary conditions along the y direction. It has to be noted that realistic samples should contain a much larger number of sites than it is possible to use in our calculations without making them incredibly time consuming. In order to reasonably simulate this in the framework of our approach, we average the results for the critical temperature over 5–10 realizations of the impurity pattern. In this subsection we present the

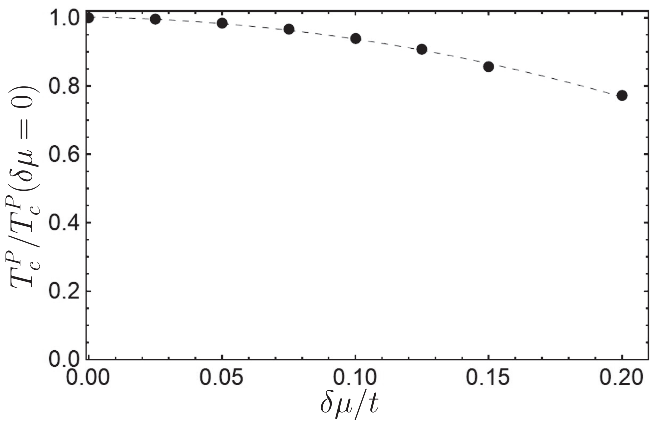

FIG. 7. General suppression of T_c due to impurities. $T_c(\phi = 0)$ is plotted as a function of the impurity strength $\delta\mu$. At the other values of misorientation angle the critical temperature demonstrates the same general trend. T_c is normalized to its value at $\delta\mu = 0$. Each point represents the averaging of the data obtained for 5–10 realizations of the random disorder restricted by a given $\delta\mu$. The dashed line is just a fit to provide a guide to eye. $\mu_S = 0.9t$, $\mu_{AF} = 0$, $h = t$, $d_{AF} = 4$, $d_S = 20$, $T_{c0} = 0.03t$.

results of Bogoliubov–de Gennes calculations of the critical temperature in the presence of impurities in the S region. Figures 7–9 show three different effects that we observed. All the results were obtained for the system with length $L = 100$ atomic layers.

The first effect, presented in Fig. 7, is the general suppression of the critical temperature with increasing of the impurity strength, reported in [38,43,44]. In this subsection we set $\mu_S = 0.9t \gg T_{c0}$. In this regime, when the chemical potential is large with respect to the superconducting energy scales, the nonmagnetic impurities in the superconductor work as effectively magnetic [38]. This results from the two sublattices and the consequent emergence of two electronic bands in the system thereby leading to the observed suppression.

Figure 8 demonstrates the gradual disappearing of the valve effect under the influence of impurities, which is

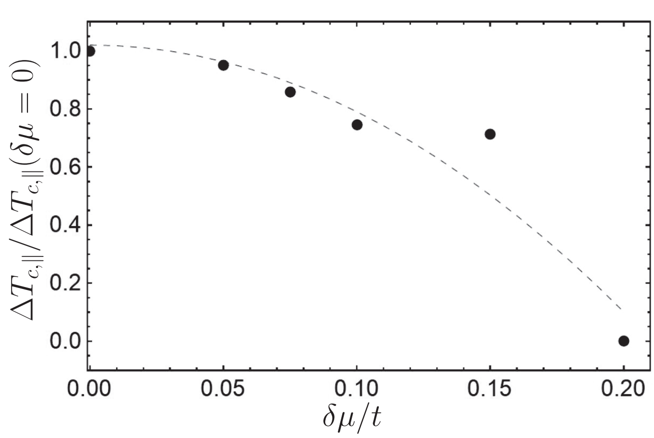

FIG. 8. Suppression of the spin-valve effect by impurities. The difference $\Delta T_{c,\parallel}$ is plotted as a function of the impurity strength $\delta\mu$. The difference is normalized to its value at $\delta\mu = 0$. All parameters are the same as in Fig. 7.

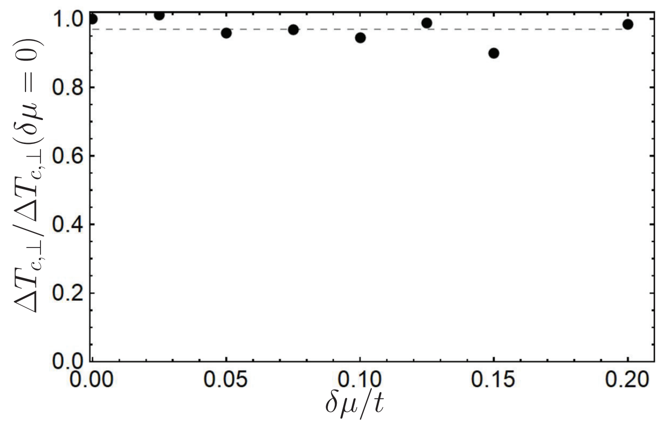

FIG. 9. $\Delta T_{c,\perp}$, normalized to its value at $\delta\mu = 0$, plotted as a function of the impurity strength $\delta\mu$. All parameters are the same as in Fig. 7.

equivalent to the decreasing value of the difference $\Delta T_{c,\parallel} = [T_c(\phi = 0) - T_c(\phi = \pi)]/2$. This is explained by the fact that the spin-valve effect is produced by the Néel triplets, which appear due to interband electron pairing [37] and therefore are suppressed by impurities.

The third effect we studied is the dependence of the depth of the dips at $T_c(\phi)$ curves at $\phi = \pi/2$ on the impurity strength, which we perform by plotting the expression $\Delta T_{c,\perp} = T_c(\phi = \pi/2) - [T_c(\phi = 0) + T_c(\phi = \pi)]/2$ as a function of $\delta\mu$. The results are presented in Fig. 9. We see that this quantity tends to be insensitive to the presence of impurities. This trend is in agreement with the physical understanding that the dip is mainly produced by the cross-product correlations f_{cross}, which are conventional (not Néel) triplets and correspond to intraband s-wave odd-frequency triplet electron pairing. Such an intraband or zero-momentum s-wave pairing is not suppressed by nonmagnetic impurities.

D. Materials

In our analysis above, we have obtained a broad picture of the spin-valve effect in the trilayer system under investigation including its dependence on the chemical potential and impurity concentration. This, in turn, provides guidance with respect to the choice of materials. The predicted spin-valve effect is the largest for superconductors with small chemical potential, as defined in our considerations above, which will harbor strong Néel correlations. Nevertheless, as it is demonstrated in this work, the spin-valve effect is also pronounced for superconductors with large chemical potential provided that the exchange field h of the AFs is strong enough. Furthermore, disorder due to impurities or interfacial lattice mismatch should be minimized. On the other hand, if one is interested in the equal-spin triplets that lead to a dip in the critical temperature around $\phi = \pi/2$, the requirements are less stringent. This is because the chemical potential can be relatively large and disorder does not play a significant role. Finally, while our theoretical considerations have focused on antiferromagnetic insulators for simplicity, one can also use metallic AFs. Having these constraints in mind, we note that our investigation is partly inspired by previous experiments observing critical temperature modifications in FeMn/Nb [45], IrMn/Nb [46], and IrMn/NbN [47] bilayers. Since these combinations produce an observable effect, they should also be good candidates for investigating our proposed trilayers.

IV. CONCLUSIONS

In this work we study AF/S/AF heterostructures with insulating antiferromagnets and fully compensated S/AF interfaces numerically by solving Bogoliubov–de Gennes equations and analytically in the framework of the quasiclassical Green's functions approach. We have demonstrated that the Néel triplet correlations lead to the dependence of superconducting critical temperature on the angle between the Néel vectors (spin-valve effect) and, in particular, to the complete suppression of superconductivity for a range of misorientation angles (absolute spin-valve effect), which is in agreement with the results presented in [36]. Our calculations confirm the previous finding of [36] that near half-filling the critical temperature is always lower for the parallel configuration of the Néel vectors than in the antiparallel $T_c^{\mathrm{P}} < T_c^{\mathrm{AP}}$, keeping in mind the new definitions of parallel and antiparallel used in this paper. It is explained by the fact that in this case the Néel triplets generated by the both interfaces are effectively summed up and strengthen each other inside the S layer. However, in this work we investigated the spin-valve effect in the full range of μ_{S} values and found that if we move away from half-filling the opposite result $T_c^{\mathrm{P}} > T_c^{\mathrm{AP}}$ can be realized depending on the width of the S layer. This behavior results from the interference of finite-momentum Néel triplet Cooper pair wave functions generated by the S/AF interfaces.

Further, we investigate cross-product equal-spin-triplet correlations f_{cross}, which appear in the AF/S/AF structure for nonaligned Néel vectors of the AFs. We provide their analytical description, prove that these correlations are of conventional (not Néel) s-wave odd-frequency type, and find parameter regions, where they are rather strong and result in the nonmonotonic dependence $T_c(\phi)$. Finally, it is shown that the presence of impurities leads to disappearing of the "$0-\pi$" spin-valve effect $\Delta T_{c,\parallel} = (T_c^{\mathrm{P}} - T_c^{\mathrm{AP}})/2$ due to the fact that impurities suppress Néel triplets. At the same time, the "perpendicular" spin-valve effect $\Delta T_{c,\perp} = T_c(\phi = \pi/2) - (T_c^{\mathrm{P}} + T_c^{\mathrm{AP}})/2$ is not suppressed by impurities, what can be considered as a proof of its origin from equal-spin cross-product triplet correlations, which should be insensitive to impurities according to their physical nature.

Therefore, our results significantly expand the current understanding of the physical processes in AF/S/AF spin valves, as well as they hopefully might inspire some new research in the area of spintronic devices based on proximity effects in superconductor/antiferromagnet hybrids.

ACKNOWLEDGMENTS

The BdG analysis was supported by the Russian Science Foundation via the RSF Project No. 22-22-00522. The calculations in the framework of the quasiclassical theory were supported by MIPT via Project No. FSMG-2023-0014. L.J.K., S.C., and A.K. acknowledge financial support from the Spanish Ministry for Science and Innovation–AEI Grant No. CEX2018-000805-M (through the "Maria de Maeztu" Programme for Units of Excellence in R&D) and Grant No. RYC2021-031063-I funded by MCIN/AEI/10.13039/501100011033 and "European Union Next Generation EU/PRTR."

APPENDIX: CALCULATION OF THE GREEN'S FUNCTION

Let us obtain the boundary condition for the normal-state Green's function at the right S/AF interface $x = d_{\mathrm{S}}/2$, which is the relation between the incident and reflected Green's functions $\check{g}_+^N(x)$ and $\check{g}_-^N(x)$. Near the right edge of the superconductor the Eilenberger equation (3) takes the form

$$[(i\omega_m\tau_z + \mu_{\mathrm{S}} - \boldsymbol{h}_r\boldsymbol{\sigma}\rho_z\tau_z a\delta(x-d_{\mathrm{S}}/2))\rho_x, \check{g}^N] + iv_{F,x}\frac{d}{dx}\check{g}^N = 0, \tag{A1}$$

which gives us the relation

$$iv(\check{g}_-^N(x=d_{\mathrm{S}}/2) - \check{g}_+^N(x=d_{\mathrm{S}}/2)) = \int_C [\boldsymbol{h}_r\boldsymbol{\sigma}a\rho_z\rho_x\tau_z\delta(x-d_{\mathrm{S}}/2), \check{g}^N]dx, \tag{A2}$$

where the integral is taken over the set $C = [d_{\mathrm{S}}/2 - \varepsilon, d_{\mathrm{S}}/2] \cup [d_{\mathrm{S}}/2, d_{\mathrm{S}}/2 - \varepsilon]$, $\varepsilon \to 0$. This leads to the boundary condition (8). The boundary condition (16) is obtained likewise from the Eilenberger equation (15) for the anomalous Green's function $\hat{f}$.

For simplifying the following calculations we analyze consequences of the symmetry of the considered system. Let us make the rotation by angle π around the axis z:

$$x \to -x, \quad y \to -y, \quad z \to z. \tag{A3}$$

After rotation (A3) different objects which are present in our problem are transformed in the following way: scalars in spin space do not change $[A(x) \to A(-x)]$, components of vectors in spin space change as $A_x(x) \to -A_x(-x)$, $A_y(x) \to -A_y(-x)$, $A_z(x) \to A_z(-x)$. Due to the symmetric choice of the coordinate axes the system itself does not change after rotation (A3), but the reflected Green's function goes to the incident one. This gives us the following relations:

$$\begin{aligned}
\check{g}_{0\alpha,-}(x) &= \check{g}_{0\alpha,+}(-x),\\
\check{g}_{x\alpha,-}(x) &= -\check{g}_{x\alpha,+}(-x),\\
\check{g}_{y\alpha,-}(x) &= -\check{g}_{y\alpha,+}(-x),\\
\check{g}_{z\alpha,-}(x) &= \check{g}_{z\alpha,+}(-x),
\end{aligned} \tag{A4}$$

where

$$\check{g}_{\beta\alpha,+(-)} \equiv \begin{pmatrix} g_{\beta\alpha,+(-)} & f_{\beta\alpha,+(-)} \\ \tilde{f}_{\beta\alpha,+(-)} & \tilde{g}_{\beta\alpha,+(-)} \end{pmatrix}. \tag{A5}$$

In the following text Green's functions without indices + (−) correspond to incident trajectories, and the reflected Green's functions can be obtained from the relations (A4).

Now let us note that the simultaneous transformation from sublattice A to sublattice B and $\boldsymbol{h} \to -\boldsymbol{h}$ does not change the system and, therefore, does not change the Green's function. Therefore, if we write $\check{g}$ in the form $\check{g} = \check{g}^0 + \check{g}^h$, where $\check{g}^0$ and $\check{g}^h$ are even and odd functions with respect to $h \to -h$, the transformation $A \leftrightarrow B$ leads to $\check{g}^0 \to \check{g}^0$ and $\check{g}^h \to -\check{g}^h$. On the other hand, the transformation $A \leftrightarrow B$ changes sign of $\rho_{y,z}$ components of the Green's function in the sublattice space, remaining $\rho_{0,x}$ components unchanged. Consequently, $\check{g}^0$ has nonzero $\rho_{0,x}$ components and $\check{g}^h$ has nonzero $\rho_{y,z}$ components. Then, from two vectors $\boldsymbol{h}_{l,r}$, which characterize our system, we can make the following basic combinations, which describe the Green's function in the spin space: $\boldsymbol{h}_l$, $\boldsymbol{h}_r$, $\boldsymbol{h}_l\boldsymbol{h}_r$, and $\boldsymbol{h}_l \times \boldsymbol{h}_r$. The first two items are odd functions with respect to $h \to -h$ and enter into the $\sigma_{y,z}$ components of the Green's function, and the second two items are even functions and enter into the $\sigma_{0,x}$ components of the Green's function. Thus, we can conclude that $\check{g}_0$ and $\check{g}_x$ have only σ_0, σ_x nonzero components in the expansion over Pauli matrices in the spin space, while $\check{g}_y$ and $\check{g}_z$ have only σ_y, σ_z nonzero components. Another consequence of the symmetry towards rotation (A3) and the structure of boundary conditions (8) and (16) is the following expanding of (A4), which can also be considered an ansatz:

$$\begin{aligned}
\check{g}_{zy,+}(x) &= \check{g}_{zy,+}(-x) = \check{g}_{zy,-}(x),\\
\check{g}_{zz,+}(x) &= -\check{g}_{zz,+}(-x) = -\check{g}_{zz,-}(x),\\
\check{g}_{yy,+}(x) &= -\check{g}_{yy,+}(-x) = \check{g}_{yy,-}(x),\\
\check{g}_{yz,+}(x) &= \check{g}_{yz,+}(-x) = -\check{g}_{yz,-}(x).
\end{aligned} \tag{A6}$$

The Eilenberger equation on the particle component $\hat{g}$ of the normal-state Green's function takes the form

$$[(i\omega_m + \mu_\mathrm{S})\rho_x, \hat{g}] + iv_{F,x}\frac{d}{dx}\hat{g} = 0 \tag{A7}$$

apart from the S/AF interfaces and can be expanded over components in the sublattice space:

$$\begin{aligned}
\frac{d}{dx}\hat{g}_0 &= 0,\\
\frac{d}{dx}\hat{g}_x &= 0,\\
2(-\omega_m + i\mu_\mathrm{S})\hat{g}_y + iv_{F,x}\frac{d}{dx}\hat{g}_z &= 0,\\
2(\omega_m - i\mu_\mathrm{S})\hat{g}_z + iv_{F,x}\frac{d}{dx}\hat{g}_y &= 0.
\end{aligned} \tag{A8}$$

As was discussed above, the components $g_{xy}, g_{xz}, g_{0y}, g_{0z}, g_{z0}, g_{zx}, g_{y0}, g_{yx}$ are equal to zero because of symmetry. Considering (A6), we write the solutions for other components:

$$\begin{aligned}
g_{00} &= \text{const},\\
g_{x0} &= \text{const},\\
g_{0x} &= \text{const},\\
g_{xx} &= \text{const},\\
g_{yy} &= iB\,\sinh \kappa x,\\
g_{zy} &= -A\,\cosh \kappa x,\\
g_{yz} &= B\,\mathrm{sgn}\, v_{F,x} \cosh \kappa x,\\
g_{zz} &= iA\,\mathrm{sgn}\, v_{F,x} \sinh \kappa x,
\end{aligned} \tag{A9}$$

where $\kappa = 2(i\mu_\mathrm{S} - \omega_m)/v$ and A, B are unknown coefficients. From the boundary condition (8) we obtain

$$\begin{aligned}
\delta g_{00} &= 0,\\
\delta g_{x0} &= -(g_{yy}(x = d_\mathrm{S}/2)\gamma_z - g_{zy}(x = d_\mathrm{S}/2)\gamma_y),\\
\delta g_{0x} &= +(g_{zz}(x = d_\mathrm{S}/2)\gamma_z + g_{yz}(x = d_\mathrm{S}/2)\gamma_y),\\
\delta g_{xx} &= 0,\\
\delta g_{yy} &= +g_{x0}(x = d_\mathrm{S}/2)\gamma_z,\\
\delta g_{zy} &= -g_{x0}(x = d_\mathrm{S}/2)\gamma_y,\\
\delta g_{yz} &= -g_{0x}(x = d_\mathrm{S}/2)\gamma_y,\\
\delta g_{zz} &= -g_{0x}(x = d_\mathrm{S}/2)\gamma_z,
\end{aligned} \tag{A10}$$

where $\gamma_{y,z} = 4iah_{y,z}/v$. Equation (A10) gives us $g_{00} = g_{xx} = 0$. Coefficients g_{x0}, g_{0x}, A, and B can be found from the normalization condition (4), which takes the form

$$A^2 + B^2 + g_{0x}^2 + g_{x0}^2 = 1, \tag{A11}$$

and substituting solutions (A9) for $g_{yy}, g_{yz}, g_{zy}, g_{zz}$ into the last four equations of the system (A10). We obtain

$$\begin{aligned}
g_{0x} &= \frac{1}{\sqrt{(1+\gamma_a^2)(1+\gamma_b^2)}},\\
g_{x0} &= \frac{\gamma_a\gamma_b}{\sqrt{(1+\gamma_a^2)(1+\gamma_b^2)}},\\
A &= \frac{\gamma_a}{\sqrt{(1+\gamma_a^2)(1+\gamma_b^2)}},\\
B &= \frac{\gamma_b}{\sqrt{(1+\gamma_a^2)(1+\gamma_b^2)}},
\end{aligned} \tag{A12}$$

where $\gamma_a = -i\gamma_z/2\,\sinh(\kappa d_\mathrm{S}/2)$, $\gamma_b = \gamma_y/2\,\cosh(\kappa d_\mathrm{S}/2)$. In the first order with respect to κd_S $\gamma_a = 2ah_z/(-\omega_m + i\mu_\mathrm{S})d_\mathrm{S}$, $\gamma_b = -2ah_y/v$.

The Eilenberger equation on the anomalous Green's function $\hat{f}$ takes the form

$$i\omega_m\{\rho_x, \hat{f}\} + \mu_\mathrm{S}[\rho_x, \hat{f}] + \Delta(\rho_x\hat{\tilde{g}} - \hat{g}\rho_x) + iv_{F,x}\frac{d}{dx}\hat{f} = 0 \tag{A13}$$

apart from the interfaces and can be expanded over components in the sublattice space:

$$\begin{aligned}
2i\omega_m\hat{f}_x + iv_{F,x}\frac{d}{dx}\hat{f}_0 &= \Delta(\hat{g}_x - \hat{\tilde{g}}_x) \equiv \hat{G}_x,\\
2i\omega_m\hat{f}_0 + iv_{F,x}\frac{d}{dx}\hat{f}_x &= \Delta(\hat{g}_0 - \hat{\tilde{g}}_0) \equiv \hat{G}_0,\\
-2i\mu_\mathrm{S}\hat{f}_z + iv_{F,x}\frac{d}{dx}\hat{f}_y &= i\Delta(\hat{g}_z + \hat{\tilde{g}}_z) \equiv \hat{G}_z,\\
2i\mu_\mathrm{S}\hat{f}_y + iv_{F,x}\frac{d}{dx}\hat{f}_z &= -i\Delta(\hat{g}_y + \hat{\tilde{g}}_y) \equiv \hat{G}_y.
\end{aligned} \tag{A14}$$

Let us expand $\hat{G}_{y,z}$ up to the first order with respect to x: $\hat{G}_{y,z} = \hat{G}^0_{y,z} + \hat{G}'_{y,z}x$. Then the general solution of (A14) is

$$\hat{f}_0 = \hat{A}\,\sinh\left(\frac{2\omega_m}{v}x\right) + \hat{B}\,\cosh\left(\frac{2\omega_m}{v}x\right) + \frac{\hat{G}_0}{2i\omega_m},$$
$$\hat{f}_x = -\hat{A}\,\cosh\left(\frac{2\omega_m}{v}x\right) - \hat{B}\,\sinh\left(\frac{2\omega_m}{v}x\right) + \frac{\hat{G}_x}{2i\omega_m},$$
$$\hat{f}_y = \hat{C}\,\sin\left(\frac{2\mu_S}{v}x\right) + \hat{D}\,\cos\left(\frac{2\mu_S}{v}x\right) + \frac{\hat{G}_y^0 + \hat{G}'_y x}{2i\mu_S} + \frac{v}{4i\mu_S^2}\hat{G}'_z,$$
$$\hat{f}_z = \hat{C}\,\cos\left(\frac{2\mu_S}{v}x\right) - \hat{D}\,\sin\left(\frac{2\mu_S}{v}x\right) - \frac{\hat{G}_z^0 + \hat{G}'_z x}{2i\mu_S} + \frac{v}{4i\mu_S^2}\hat{G}'_y, \tag{A15}$$

where $\hat{A}, \hat{B}, \hat{C}, \hat{D}$ are 2×2 spin matrices of unknown coefficients. $f_{0y}, f_{0z}, f_{xy}, f_{xz}, f_{y0}, f_{yx}, f_{z0}, f_{zx}$ are equal to zero due to symmetry, and for other components we obtain in the linear order with respect to x:

$$f_{00} = A_0\frac{2\omega_m}{v}x\,\mathrm{sgn}\,v_{F,x} + B_0 + \frac{G_{00}}{2i\omega_m},$$
$$f_{0x} = -A_0 - B_0\frac{2\omega_m}{v}x\,\mathrm{sgn}\,v_{F,x} + \frac{G_{0x}}{2i\omega_m},$$
$$f_{x0} = A_x\frac{2\omega_m}{v}x + \left(B_x + \frac{G_{x0}}{2i\omega_m}\right)\mathrm{sgn}\,v_{F,x},$$
$$f_{xx} = \left(-A_x + \frac{G_{xx}}{2i\omega_m}\right)\mathrm{sgn}\,v_{F,x} - B_x\frac{2\omega_m}{v}x,$$
$$f_{yy} = \left(C_y\frac{2\mu_S}{v} + \frac{G'_{yy}}{2i\mu_S}\right)x + D_y\,\mathrm{sgn}\,v_{F,x} + \left(G^0_{yy} + \frac{v}{2\mu_S}G'_{yz}\right)\frac{\mathrm{sgn}\,v_{F,x}}{2i\mu_S},$$
$$f_{yz} = C_y\,\mathrm{sgn}\,v_{F,x} - \left(D_y\frac{2\mu_S}{v} + \frac{G'_{yz}}{2i\mu_S}\right)x + \left(-G^0_{yz} + \frac{v}{2\mu_S}G'_{yy}\right)\frac{\mathrm{sgn}\,v_{F,x}}{2i\mu_S},$$
$$f_{zy} = \left(C_z\frac{2\mu_S}{v} + \frac{G'_{zy}}{2i\mu_S}\right)x\,\mathrm{sgn}\,v_{F,x} + D_z + \left(G^0_{zy} + \frac{v}{2\mu_S}G'_{zz}\right)\frac{1}{2i\mu_S},$$
$$f_{zz} = C_z - \left(D_z\frac{2\mu_S}{v} + \frac{G'_{zz}}{2i\mu_S}\right)x\,\mathrm{sgn}\,v_{F,x} + \left(-G^0_{zz} + \frac{v}{2\mu_S}G'_{zy}\right)\frac{1}{2i\mu_S}, \tag{A16}$$

where we have used the expansions $\hat{A} = \sum_\alpha \sigma_\alpha A_\alpha$, $\hat{B} = \sum_\alpha \sigma_\alpha B_\alpha$, $\hat{C} = \sum_\alpha \sigma_\alpha C_\alpha$, $\hat{D} = \sum_\alpha \sigma_\alpha D_\alpha$, $\hat{G}_\beta = \sum_\alpha \sigma_\alpha G_{\alpha\beta}$. The solution for the normal Green's function gives us $G'_{yz} = G'_{zy} = G^0_{yy} = G^0_{zz} = G_{00} = G_{xx} = 0$, and the relations (A6) lead to $B_0 = A_x = D_y = C_z = 0$. Other unknown coefficients are found from the boundary condition (16):

$$A_0 = \frac{i\{G'_{zz}h_z a v^4 + 4\mu_S[v^2(G^0_{zy}h_z a v + d_S G^0_{yz}h_y a\mu_S) - 2G_{x0}h_y h_z a^2(v^2 + d_S^2\mu_S^2)]\}}{4d_S v^3\mu_S^2\omega_m},$$
$$B_x = \frac{iG_{x0}}{2\omega_m},$$
$$C_y = \frac{i[G'_{yy}v^3 + 2\mu_S(-G^0_{yz}v^2 + 2d_S G_{x0}h_z a\mu_S)]}{4v^2\mu_S^2},$$
$$D_z = \frac{i(G'_{zz}v^2 + 8G_{x0}h_y a\mu_S)}{8v\mu_S^2}. \tag{A17}$$

[1] A. I. Buzdin, Proximity effects in superconductor-ferromagnet heterostructures, Rev. Mod. Phys. **77**, 935 (2005).

[2] F. S. Bergeret, A. F. Volkov, and K. B. Efetov, Odd triplet superconductivity and related phenomena in superconductor-ferromagnet structures, Rev. Mod. Phys. **77**, 1321 (2005).

[3] M. Eschrig, Spin-polarized supercurrents for spintronics: a review of current progress, Rep. Prog. Phys. **78**, 104501 (2015).

[4] J. Linder and J. W. A. Robinson, Superconducting spintronics, Nat. Phys. **11**, 307 (2015).

[5] P. De Gennes, Coupling between ferromagnets through a superconducting layer, Phys. Lett. **23**, 10 (1966).

[6] B. Li, N. Roschewsky, B. A. Assaf, M. Eich, M. Epstein-Martin, D. Heiman, M. Münzenberg, and J. S. Moodera, Superconducting spin switch with infinite magnetoresistance induced by an internal exchange field, Phys. Rev. Lett. **110**, 097001 (2013).

[7] S. Oh, D. Youm, and M. R. Beasley, A superconductive magnetoresistive memory element using controlled exchange interaction, Appl. Phys. Lett. **71**, 2376 (1997).

[8] L. R. Tagirov, Low-field superconducting spin switch based on a superconductor /ferromagnet multilayer, Phys. Rev. Lett. **83**, 2058 (1999).

[9] Y. V. Fominov, A. A. Golubov, and M. Y. Kupriyanov, Triplet proximity effect in FSF trilayers, JETP Lett. **77**, 510 (2003).

[10] I. C. Moraru, W. P. Pratt, and N. O. Birge, Magnetization-dependent T_c shift in ferromagnet/superconductor/ferromagnet trilayers with a strong ferromagnet, Phys. Rev. Lett. **96**, 037004 (2006).

[11] A. Singh, C. Sürgers, and H. v. Löhneysen, Superconducting spin switch with perpendicular magnetic anisotropy, Phys. Rev. B **75**, 024513 (2007).

[12] Y. V. Fominov, A. A. Golubov, T. Y. Karminskaya, M. Y. Kupriyanov, R. G. Deminov, and L. R. Tagirov, Superconducting triplet spin valve, JETP Lett. **91**, 308 (2010).

[13] J. Zhu, I. N. Krivorotov, K. Halterman, and O. T. Valls, Angular dependence of the superconducting transition temperature in ferromagnet-superconductor-ferromagnet trilayers, Phys. Rev. Lett. **105**, 207002 (2010).

[14] C.-T. Wu and O. T. Valls, Superconducting proximity effects in ferromagnet/superconductor heterostructures, J. Supercond. Nov. Magn. **25**, 2173 (2012).

[15] P. V. Leksin, N. N. Garif'yanov, I. A. Garifullin, Y. V. Fominov, J. Schumann, Y. Krupskaya, V. Kataev, O. G. Schmidt, and B. Büchner, Evidence for triplet superconductivity in a superconductor-ferromagnet spin valve, Phys. Rev. Lett. **109**, 057005 (2012).

[16] N. Banerjee, C. B. Smiet, R. G. J. Smits, A. Ozaeta, F. S. Bergeret, M. G. Blamire, and J. W. A. Robinson, Evidence for spin selectivity of triplet pairs in superconducting spin valves, Nat. Commun. **5**, 3048 (2014).

[17] A. A. Jara, C. Safranski, I. N. Krivorotov, C.-T. Wu, A. N. Malmi-Kakkada, O. T. Valls, and K. Halterman, Angular dependence of superconductivity in superconductor/spin-valve heterostructures, Phys. Rev. B **89**, 184502 (2014).

[18] A. Singh, S. Voltan, K. Lahabi, and J. Aarts, Colossal proximity effect in a superconducting triplet spin valve based on the half-metallic ferromagnet CrO_2, Phys. Rev. X **5**, 021019 (2015).

[19] A. A. Kamashev, N. N. Garif'yanov, A. A. Validov, J. Schumann, V. Kataev, B. Büchner, Y. V. Fominov, and I. A. Garifullin, Superconducting spin-valve effect in heterostructures with ferromagnetic heusler alloy layers, Phys. Rev. B **100**, 134511 (2019).

[20] K. Westerholt, D. Sprungmann, H. Zabel, R. Brucas, B. Hjörvarsson, D. A. Tikhonov, and I. A. Garifullin, Superconducting spin valve effect of a V layer coupled to an antiferromagnetic [Fe/V] superlattice, Phys. Rev. Lett. **95**, 097003 (2005).

[21] G. Deutscher and F. Meunier, Coupling between ferromagnetic layers through a superconductor, Phys. Rev. Lett. **22**, 395 (1969).

[22] J. Y. Gu, C.-Y. You, J. S. Jiang, J. Pearson, Y. B. Bazaliy, and S. D. Bader, Magnetization-orientation dependence of the superconducting transition temperature in the ferromagnet-superconductor-ferromagnet system: CuNi/Nb/CuNi, Phys. Rev. Lett. **89**, 267001 (2002).

[23] Y. Gu, G. B. Halász, J. W. A. Robinson, and M. G. Blamire, Large superconducting spin valve effect and ultrasmall exchange splitting in epitaxial rare-earth-niobium trilayers, Phys. Rev. Lett. **115**, 067201 (2015).

[24] T. Y. Karminskaya, A. A. Golubov, and M. Y. Kupriyanov, Anomalous proximity effect in spin-valve superconductor/ferromagnetic metal/ferromagnetic metal structures, Phys. Rev. B **84**, 064531 (2011).

[25] O. T. Valls, *Superconductor/Ferromagnet Nanostructures An Illustration of the Physics of Hybrid Nanomaterials*, Lecture Notes in Physics (World Scientific, Singapore, 2022).

[26] C.-T. Wu, O. T. Valls, and K. Halterman, Tunneling conductance and spin transport in clean ferromagnet/ferromagnet/superconductor heterostructures, Phys. Rev. B **90**, 054523 (2014).

[27] K. Halterman, O. T. Valls, and C.-T. Wu, Charge and spin currents in ferromagnetic josephson junctions, Phys. Rev. B **92**, 174516 (2015).

[28] E. Moen and O. T. Valls, Transport in ferromagnet/superconductor spin valves, Phys. Rev. B **95**, 054503 (2017).

[29] E. Moen and O. T. Valls, Spin current and spin transfer torque in ferromagnet/superconductor spin valves, Phys. Rev. B **97**, 174506 (2018).

[30] E. Moen and O. T. Valls, Quasiparticle conductance in spin valve josephson structures, Phys. Rev. B **101**, 184522 (2020).

[31] E. V. Gomonay and V. M. Loktev, Spintronics of antiferromagnetic systems (review article), Low Temp. Phys. **40**, 17 (2014).

[32] V. Baltz, A. Manchon, M. Tsoi, T. Moriyama, T. Ono, and Y. Tserkovnyak, Antiferromagnetic spintronics, Rev. Mod. Phys. **90**, 015005 (2018).

[33] T. Jungwirth, X. Marti, P. Wadley, and J. Wunderlich, Antiferromagnetic spintronics, Nat. Nanotechnol. **11**, 231 (2016).

[34] A. Kamra, A. Rezaei, and W. Belzig, Spin splitting induced in a superconductor by an antiferromagnetic insulator, Phys. Rev. Lett. **121**, 247702 (2018).

[35] A. Brataas, B. van Wees, O. Klein, G. de Loubens, and M. Viret, Spin insulatronics, Phys. Rep. **885**, 1 (2020).

[36] L. J. Kamra, S. Chourasia, G. A. Bobkov, V. M. Gordeeva, I. V. Bobkova, and A. Kamra, Complete T_c suppression and néel triplets mediated exchange in antiferromagnet-superconductor-antiferromagnet trilayers, Phys. Rev. B **108**, 144506 (2023).

[37] G. A. Bobkov, I. V. Bobkova, A. M. Bobkov, and A. Kamra, Néel proximity effect at antiferromagnet/superconductor interfaces, Phys. Rev. B **106**, 144512 (2022).

[38] G. A. Bobkov, I. V. Bobkova, and A. M. Bobkov, Proximity effect in superconductor/antiferromagnet hybrids: Néel triplets and impurity suppression of superconductivity, Phys. Rev. B **108**, 054510 (2023).

[39] G. A. Bobkov, I. V. Bobkova, and A. A. Golubov, Magnetic anisotropy of the superconducting transition in superconductor/antiferromagnet heterostructures with spin-orbit coupling, Phys. Rev. B **108**, L060507 (2023).

[40] S. Chourasia, L. J. Kamra, I. V. Bobkova, and A. Kamra, Generation of spin-triplet cooper pairs via a canted antiferromagnet, Phys. Rev. B **108**, 064515 (2023).

[41] G. A. Bobkov, V. M. Gordeeva, A. M. Bobkov, and I. V. Bobkova, Oscillatory superconducting transition temperature in superconductor/antiferromagnet heterostructures, Phys. Rev. B **108**, 184509 (2023).

[42] J. Zhu, *Bogoliubov-de Gennes Method and Its Applications*, Lecture Notes in Physics (Springer, Berlin, 2016).

[43] A. I. Buzdin and L. N. Bulaevskiĭ, Antiferromagnetic superconductors, Sov. Phys. Usp. **29**, 412 (1986).

[44] E. H. Fyhn, A. Brataas, A. Qaiumzadeh, and J. Linder, Superconducting proximity effect and long-ranged triplets in dirty metallic antiferromagnets, Phys. Rev. Lett. **131**, 076001 (2023).

[45] C. Bell, E. J. Tarte, G. Burnell, C. W. Leung, D.-J. Kang, and M. G. Blamire, Proximity and josephson effects in superconductor/antiferromagnetic $Nb/\gamma - Fe_{50}Mn_{50}$ heterostructures, Phys. Rev. B **68**, 144517 (2003).

[46] B. L. Wu, Y. M. Yang, Z. B. Guo, Y. H. Wu, and J. J. Qiu, Suppression of superconductivity in NB by IRMN in IrMn/Nb bilayers, Appl. Phys. Lett. **103**, 152602 (2013).

[47] R. L. Seeger, G. Forestier, O. Gladii, M. Leiviskä, S. Auffret, I. Joumard, C. Gomez, M. Rubio-Roy, A. I. Buzdin, M. Houzet, and V. Baltz, Penetration depth of cooper pairs in the irmn antiferromagnet, Phys. Rev. B **104**, 054413 (2021).